Supporting Information

Quasi-solid electrolyte developed on hierarchical rambutan-like γ-AlOOH microspheres with high ionic conductivity for lithium ion batteries

Mengmeng Gao[a], Xiaolei Wu[a], Shuhong Yi[a], Shuwei Sun[a], Caiyan Yu[a], Dong Yan[b], Hui Ying Yang[b], Huiling Zhao[a] and Ying Bai*[a]*

[a]International Joint Research Laboratory of New Energy Materials and Devices of Henan Province, School of Physics and Electronics, Henan University, Kaifeng, 475004, P. R. China

[b]Pillar of Engineering Product Development, Singapore University of Technology and Design, Singapore 487372, Singapore

***Corresponding author.**

E-mail: zhao@henu.edu.cn (H. L. Zhao); ybai@henu.edu.cn (Y. Bai)

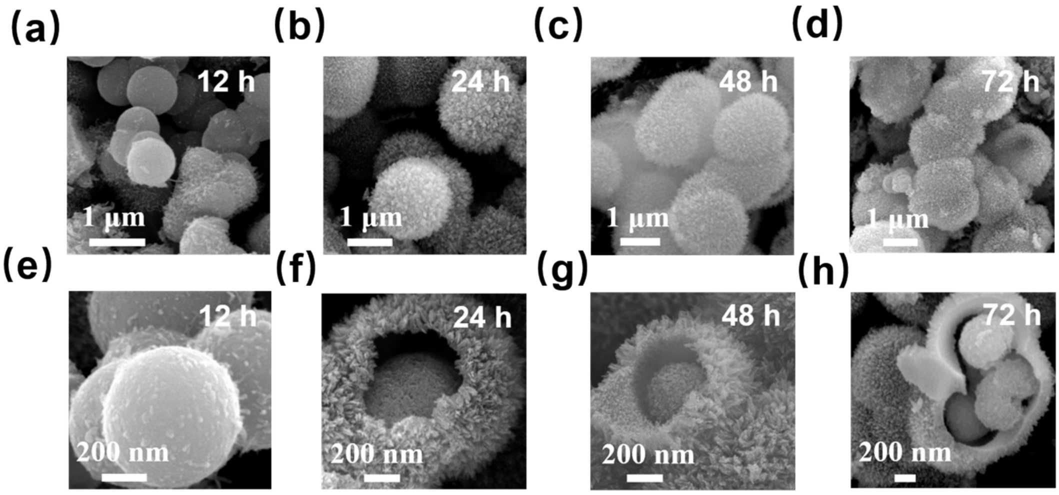

Fig. S1 SEM images for the products at different reaction times.

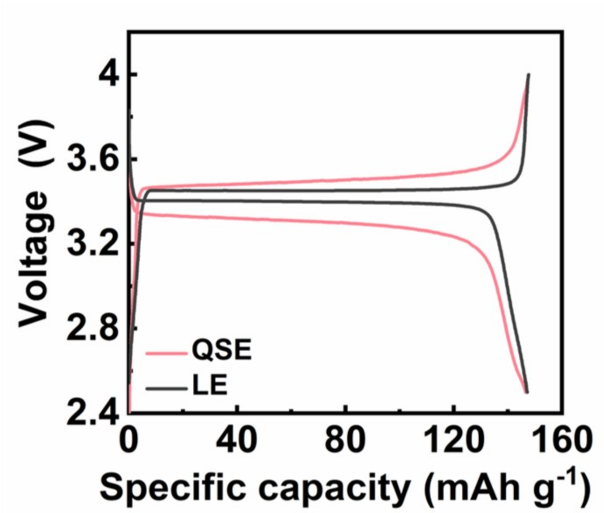

Fig. S2 The initial charge/discharge profiles of LFP/γ-AlOOH-QSE/Li and LFP/QSE/Li cells.

The initial discharge specific capacities of the LFP/γ-AlOOH-QSE/Li and LFP/LE/Li cells are similar at 0.1 C (146.6 *vs.* 147.1 mAh g^{-1}), though the latter one exhibits slightly a higher capacity retention (99.3% *vs.* 99.7%).

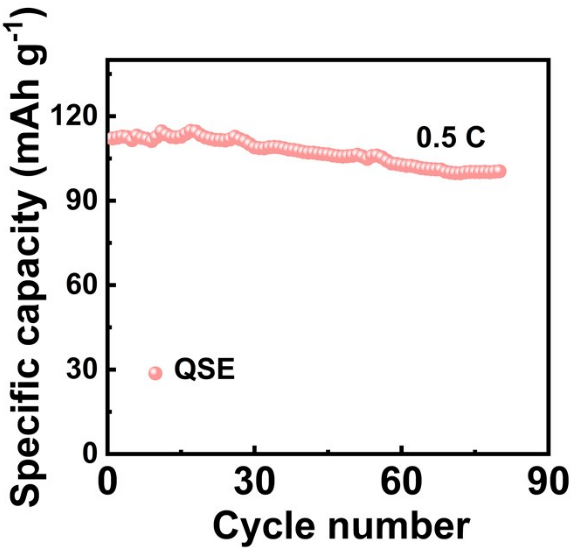

Fig. S3 Cycling performance of the assembled LFP/γ-AlOOH-QSE/Li cell at 0.5 C.

Although the specific capacity of LFP/AlOOH-QSE/Li degrades faster at high current rate compared with that of LE (Fig. 2b), the capacity retention could still be remained 95.6% after 80 cycles under high current density of 0.5 C.

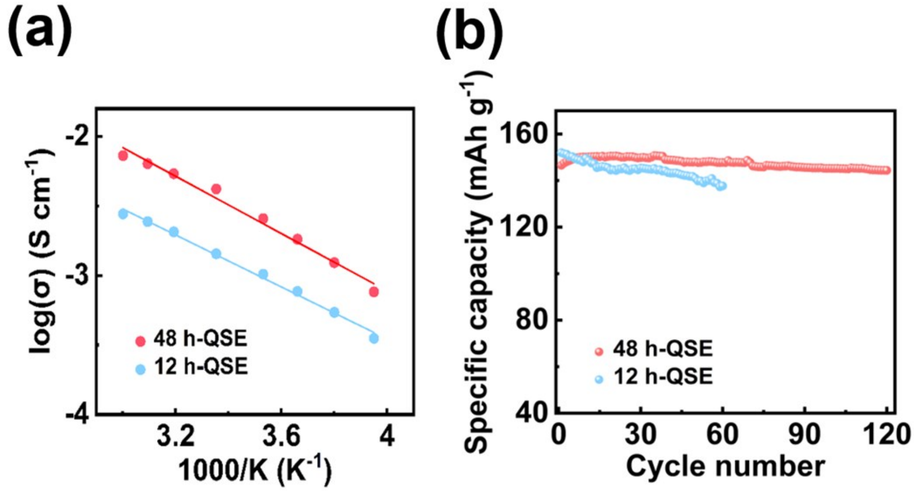

Fig. S4 (a) Ionic conductivities of 48 h-QSE, 12 h-QSE symmetrical cells within the temperature range of –20–80 ℃; (b) Cycling performances of the assembled cells with 48 h-QSE and 12 h-QSE as electrolytes.

According to Fig. S4b, long-term cycling performance of the assembled cells with 48 h-QSE electrolytes is better than that with 12 h-QSE, further verifying the important influence of morphologies of γ-AlOOH microspheres on the properties of QSE materials.

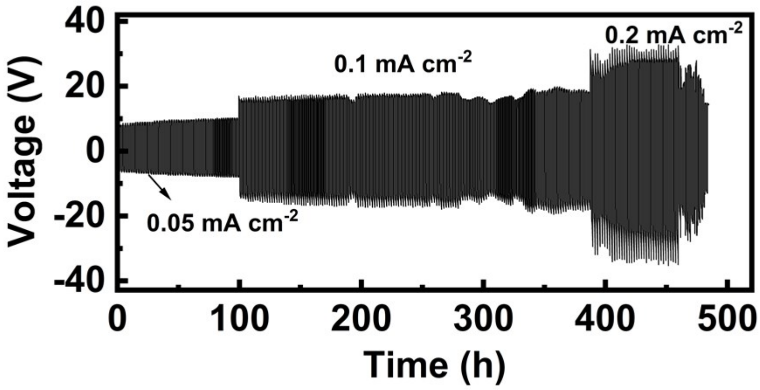

Fig. S5 Time-dependent voltage profiles for lithium plating/striping experiment for Li/LE/Li symmetric coin cell under the current densities of 0.05, 0.1, and 0.2 mA cm^{-2}.

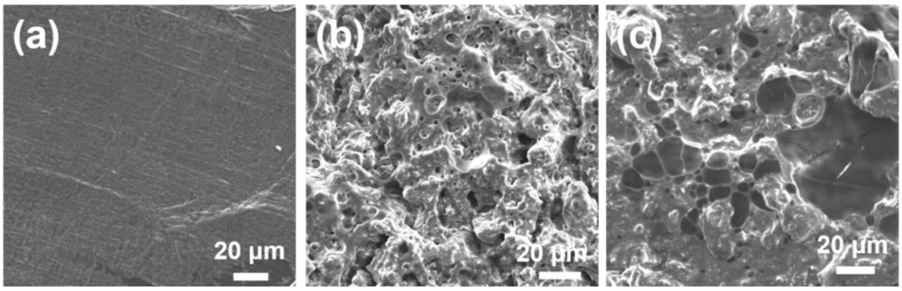

Fig. S6 Surface morphologies of Li anodes. (a) The fresh pristine Li anode; (b) LFP/γ-AlOOH-QSE/Li cell; (c) Conventional LFP cell with LE.

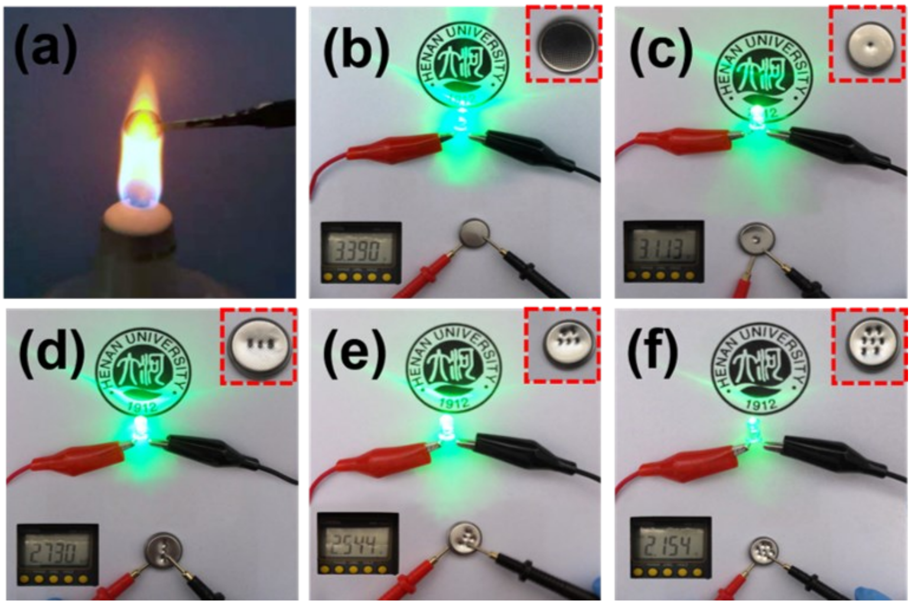

Fig. S7 (a) Combustion test of the γ-AlOOH-QSE sheet; (b-f) Illustration of lighting LED lamp under continuous puncture treatment.

Table S1 Impedances values for assembled LFP/γ-AlOOH-QSE/Li cell at different cycles under 0.1 C.

	20th	**60th**	**100th**
R_{ct} (Ω)	2489	2858	3030
W_1(Ω)	81	78	83

Table S2 The ionic conductivities of previously proposed QSEs.

QSE	**Ionic conductivity (S cm^{-1})**	**Ref.**
hollow silica (HS)	2.50×10^{-3} (25 °C)	1
ZIF-8	1.05×10^{-4} (25 °C)	2
Porous molecular cage	1.00×10^{-3} (25 °C)	3
$Mg_2B_2O_5$/PEO	1.53×10^{-4} (40 °C)	4
$Li_{1.3}Al_{0.3}Ti_{1.7}(PO_4)_3$	8.05×10^{-5} (25 °C)	5
MCM-41	6.37×10^{-4} (30 °C)	6
SiO_2	1.74×10^{-4} (25 °C)	7
γ-Al_2O_3	1.10×10^{-3} (25 °C)	8
MOF	3.10×10^{-4} (25 °C)	9
PVDF-HFP/Al_2O_3	1.00×10^{-3} (25 °C)	10
PVDF-PEO/$Li_{1.4}Al_{0.4}Ti_{1.6}(PO_4)_3$	5.24×10^{-4} (25 °C)	11
PAN/$Li_{1.4}Al_{0.4}Ti_{1.6}(PO_4)_3$	6.50×10^{-4} (60 °C)	12
SSZ-13/PEO	1.91×10^{-4} (60 °C)	13
COF/$LiClO_4$	0.26×10^{-3} (25 °C)	14
γ-AlOOH-QSE	4.00×10^{-3} (25 °C)	**This work**
PVDF-HFP /$Li_7La_3Zr_2O_{12}$	1.10×10^{-4} (25 °C)	15

References

1 J. S. Zhang, Y. Bai. X. G. Sun, Y. C. Li, B. K. Guo, J. H. Chen, G. M. Veith, D. K. Hensley, M. P. Paranthaman, John B. Goodenough and S. Dai *Nano Lett.*, 2015, **15**, 3398-3402.

2 C. Sun, J. h. Zhang. X. F. Yuan, J. N. Duan, S. W. Deng, J. M. Fan, J. K. Chang, M. S. Zheng, and Q. F. Dong, *ACS Appl. Mater. Interfaces*, 2019, **11**, 46671-46677.

3 A. Petronico,T. P. Moneypenny, Bruno G. Nicolau, Jeffrey S. Moore, Ralph G. Nuzzo, and Andrew. A. Gewirth, *J. Am. Chem. Soc.*, 2018, **140**, 7504-7509.

4 O. Sheng, C. B. Jin, J. M. Luo, H. D Yuan, H. Huang, Y. P. Gan, J. Zhang, Y. Xia, C. Liang, W. K. Zhang, and X. Y. Tao, *Nano Lett.*, 2018, **18**, 3104-3112.

5 Y. L. Liu, J. R. Liu. Q. Sun, D. W. Wang, K. R. Adair, J. N. Liang, C. Zhang, L. Zhang, S. G. Lu, H.

Huang, X. Song, and X. L. Sun, *ACS Appl. Mater.* Interfaces, 2019, **11**, 27890-27896.
6 A. K. Tripathi, R. K. Singh, *J. Energy Storage*, 2018, **15**, 283-291.
7 D. Zhou, R. Liu, Y. B. He, F. Li, M. Liu, B. Li, Q. H. Yang, Q. Cai and F. Kang, *Adv. Energy Mater.*, 2016, **6**, 1502214.
8 T. H. Xu, J. Sun, S. Yi, D. Wang, Y. Li, Q. Pei, D. Pan, H. Zhao and Y. Bai, *Solid State Ionics*, 2018, **326**, 110-115.
9 B. M. Wiers, M. L. Foo, Nitash P. Balsara, and Jeffrey R. Long, *J. Am. Chem. Soc.*, 2011, **133**, 14522-14525.
10 Y. K. Zheng, Y. Tu , Y. Y. Lu and Lynden A. Arche, *Adv. Energy Mater.*, 2014, **4**.
11 S. Yi, T. Xu, L. Li, M. Gao, K. Du, H. Zhao and Y. Bai, *Solid State Ionics*, 2020, **355**, 115419.
12 D. Li, L. Chen. S. Wang, and L. Z. Fan, *ACS Appl. Mater. Interfaces*, 2018, **10**, 7069-7078.
13 W. Li, S. Zhang, B. G. Wang, S. Gu, D. Xu, J. Wang, C. H. Chen, and Z. Y. Wen, *ACS Appl. Mater. Interfaces*, 2018, **10**, 23874-23882.
14 D. A. Vazquez Molina, G. S. Mohammad. Pour, C. Lee, M. W. Logan, X. F. Duan, James K. Harper, and Fernando J. Uribe Romo, *J. Am. Chem. Soc.*, 2016, **138**, 9767-9770.
15 W. Zhang, J. Nie, F. Li, Z. L. Wang and C. Sun, *Nano*, 2018, **45**, 413-419.